2018

An energy saving variable damping seat suspension system with regeneration capability

Donghong Ning
University of Wollongong, dn654@uowmail.edu.au

Haiping Du
University of Wollongong, hdu@uow.edu.au

Shuaishuai Sun
University of Wollongong, ss886@uowmail.edu.au

Wenfei Li
University of Wollongong, wl015@uowmail.edu.au

Weihua Li
University of Wollongong, weihuali@uow.edu.au

An energy saving variable damping seat suspension system with regeneration capability

Abstract

In this paper, an energy saving variable damping seat suspension system is designed, manufactured and validated. A controllable electromagnetic damper (EMD), which consists of a permanent magnet synchronous motor (PMSM), a 3-phase rectifier, a metal-oxide-semiconductor field-effect transistor (MOSFET) switch module, an external resistor, a diode, and a capacitor, is designed and tested firstly. The EMD is integrated with a planetary gearbox to amplify its torque output, and both of them are installed on the centre of the scissors structure of a seat suspension. The EMD's damping property can be controlled by exerting pulse width modulation (PWM) signal with different duty cycles on the MOSFET switch module. By analysing the EMD test results and the seat suspension's kinematic, the controllable damping of the EMD is derived from 115.68 Ns/m to 669.74 Ns/m. A control method for vibration isolation is proposed considering that the generated damping force is reverse to the suspension's relative velocity, and its value is related to both the damping coefficient and the relative velocity, thus the desired control force can be partially achieved by the variable damper. The proposed variable damping seat suspension and its controller are validated on a 6-degree of freedom (6-DOF) vibration platform in both frequency domain and time domain.

Disciplines

Engineering | Science and Technology Studies

Publication Details

D. Ning, H. Du, S. Sun, W. Li & W. Li, "An energy saving variable damping seat suspension system with regeneration capability," IEEE Transactions on Industrial Electronics, vol. 65, (10) pp. 8080-8091, 2018.

An energy saving variable damping seat suspension system with regeneration capability

Donghong Ning, Haiping Du, *Member, IEEE,* Shuaishuai Sun, Wenfei Li, Weihua Li, *Member, IEEE*

***Abstract*—In this paper, an energy saving variable damping seat suspension system is designed, manufactured, modelled and validated. A continuously controllable electromagnetic damper (EMD) system, which consists of a permanent magnet synchronous motor (PMSM), a three-phase rectifier, a metal-oxide-semiconductor field-effect transistor (MOSFET) switch and an external resistor, is built and tested firstly. Its model parameters have been identified based on the test results. The EMD's damping property can be controlled by exerting pulse width modulation (PWM) signal with different duty cycles on the MOSFET switch. The EMD is integrated with a planetary gearbox to amplify its torque output, and the formed variable damper is installed on the centre of the scissors structure of a seat suspension. By analysing the EMD test results and the seat suspension's kinematic, the controllable damping of the proposed seat suspension is known as from 112 Ns/m to 746 Ns/m. A control method for vibration isolation is proposed based on the system model. The proposed variable damping seat suspension and its controller are validated on a 6-degree of freedom (6-DOF) vibration platform in both frequency domain and time domain; a well tuned commercial passive seat suspension is also tested for comparison. The test results show that the controlled variable damping seat suspension has better performance in vibration isolation than the proposed seat with highest and lowest damping, and the conventional passive one. In the meantime, the RMS value of the system harvestable power is 1.492 W, and the power consumption of the PWM control signal is very few. Therefore, this variable damping seat suspension can improve the ride comfort with ignorable energy cost.**

***Index Terms*—seat suspension; vibration control; variable damping; regenerative; energy saving.**

Manuscript received August 26, 2017; revised November 26, 2017 and January 05, 2018; accepted January 18, 2018. This work was supported in part by the Australian Research Council's Linkage Projects funding scheme (project number LP160100132), the University of Wollongong and China Scholarship Council joint scholarships (201306300043).

D. Ning, H. Du and W. Li are with the School of Electrical, Computer and Telecommunications Engineering, University of Wollongong, Wollongong, N.S.W. 2522, Australia (e-mail: dning@uow.edu.au hdu@uow.edu.au; wl015@uowmail.edu.au).

S. Sun and W. Li are with the School of Mechanical, Material, Mechatronics and Biomedical Engineering, University of Wollongong, Wollongong, N.S.W. 2522, Australia (e-mail: ssun@uow.edu.au; weihuali@uow.edu.au).

I. INTRODUCTION

Long-term exposure to vibration will cause health problems, such as lower back pain [1]; especially for heavy duty vehicle drivers, severe vibration is transmitted to the driver body, due to the uneven road condition. Vehicle seat suspension system is widely adopted for improving drivers' ride comfort and protecting their health. Both active and semi-active seat suspension systems have been proposed to effectively deal with those vibrations. However, energy consumption issue of these two kinds of suspension systems also needs to be considered. The energy saving or regenerative seat suspension systems should be developed to reduce the possible energy consumption while providing ride comfort.

Three kinds of seat suspensions have been extensively studied, namely, passive, semi-active and active seat suspensions. A negative stiffness seat suspension is proposed for a passive seat suspension to have better performance in resonance frequency [2]. The active seat suspensions has been proposed with different actuators, such as the electromagnetic linear actuator [3], the hydraulic absorber [4], the pneumatic actuator [5] and the rotary motor [6-8]. The active seat suspension has best performance in improving ride comfort, but the high energy consumption is the main issue for its application. Thus, the semi-active seat suspension is proposed, which consumes much less power but has an acceptable performance. The linear electrorheological (ER) fluid damper and the magnetorheological (MR) fluid damper have been proposed for seat suspension [9, 10]. A rotary MR damper is designed for a heavy duty vehicle seat in [11]. An MR damper has been applied in the helicopter crew seat to enhance occupant comfort [12]. Though the traditional semi-active seat suspension consumes less power than the active one, it still needs energy input; for example, in order to control an MR damper, the maximum control current for a coil composed by the winding copper wire can reach to 1 A in [11]. In order to further save energy, the semi-active seat suspension is worth of more attention.

Electromagnetic damper (EMD), instead of consuming energy, can harvest energy from road vibration, and the regenerative vehicle suspension has been studied recently [13-17]. Generally, a rotary motor or a linear one is applied in those suspensions. When the rotary motor is used, the

transmission devices (from linear motion to rotary one), such as rack and pinion, are required [18, 19]. The linear generator can directly harvest the vibration energy [20-22], but, with a given space, the rotary one can generate more power [23]. For their promising prospect, the study of regeneration suspensions should be combined with the energy harvesting and vibration control [24]. The damping of the EMD can be changed by replacing its external loads (resistors) [18, 25]; this characteristic can be applied in vibration control. In addition, the EMDs are designed with MR or ER dampers [26, 27] in order to increase the output damping force. However, the continuously real-time control of an EMD system to enhance its performance in vibration isolation while regenerating energy has not been fully studied. In [28], an analysis and evaluation methodology for the regenerative brake is proposed, which is also applicable for the EMD damper system.

In this paper, an implementable variable damping EMD system is designed, built and modelled; it can continuously change its damping in real-time by controlling a metal-oxide-semiconductor field-effect transistor (MOSFET) switch with pulse width modulation (PWM) signal. The main component of the proposed damping controllable EMD system is a three-phase permanent magnet synchronous motor (PMSM), thus, it can be built with low price; at the same time, the system maintenance can be easily implemented due to its concise circuit. Based on the controllable EMD, a variable damping seat suspension prototype is designed; it can be effortlessly manufactured from the modification of a conventional passive seat suspension. By applying the scissors structure in the seat suspension, no additional transmission devices are required. The main contributions of this paper are listed as:

- A novel energy saving semi-active seat suspension is proposed with an EMD of which damping can be continuously controlled by the PWM signal. The consumed energy by the PWM signal is ignorable, and the seat suspension has the regeneration capability.
- The seat suspension model including the EMD system is derived, and the model parameters are identified with experimental tests.
- A controller implementation methodology has been proposed for vibration isolation of the seat suspension. And the vibration experiments are conducted to validate the effectiveness of the proposed system.

This seat suspension can greatly improve the ride comfort in the practical applications.

The rest of the paper is organised as following: Section II presents the variable damping seat suspension system; Section III implements the variable damping test and parameter identification; the controller design is shown in Section IV; the experimental evaluations are presented in Section V; Finally, Section VI presents the conclusions of this research.

Notation: I is used to denote the identity matrix of appropriate dimensions. * is used to represent a term that is induced by symmetry.

II. DAMPING CONTROLLABLE EMD AND TEST

This section proposes an implementable method to continuously control the damping of an EMD in real time with very few energy consumption which can be even ignored considering its regeneration capability. A prototype is manufactured and the system model is built. Then, the system is comprehensively tested and its parameters are identified.

A. Damping controllable EMD system

The controllable EMD system prototype is shown in Figure 1 and its schematic diagram is shown in Figure 2. In the system, a 3-phase PMSM, which can be modelled as three back electromotive force (EMF) voltages (e_a, e_b, e_c), three internal resistors (R_{ia}, R_{ib}, R_{ic}) and three internal inductors (L_{ia}, L_{ib}, L_{ic}), is utilised; a three-phase rectifier is applied to transfer the generated alternating current (AC) to direct current (DC); a MOSFET (STP60NF06) switch is controlled by a 10 V PWM signal; R_e is an external resistor and it can be replaced by an energy storage circuit. The applied PMSM is a Panasonic motor (MSMJ042G1U). The applied N-channel MOSFET has an insulated gate, whose voltage determines the conductivity of the device; when a 10 V voltage is exerted on the Gate pin, the resistance between the Drain and Source pins are 0 Ohm ideally; when a 0 V voltage is applied, the circuit is open.

The working principle of the system is intuitive. The damping of an EMD is increasing with the decrease of its external loads [18]. When the input PWM signal is in 10 V state, the MOSFET switch is on, then the positive and negative terminals of the three-phase rectifier are shorted, which is equivalent to that a 0 Ohm external resistor is applied to the EMD, and in this scenario, the EMD has its biggest damping. On the contrary, when the input PWM signal is in 0 V state, the MOSFET switch is off, then the damping of the EMD is determined by the external resistor R_e. In this paper, a 40 Ohm resistor is used as the external load which can determine the smallest damping of the EMD. Thus, the damping of the EMD can be varied between its smallest and biggest values, when the high frequency PWM signal (4000 Hz in this paper) is implemented with different duty cycle values.

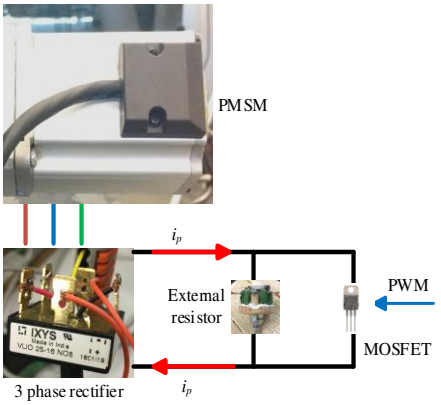

Figure 1. Controllable EMD system prototype.

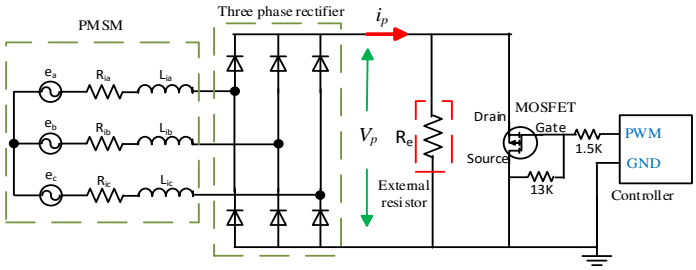

Figure 2. Controllable EMD system schematic diagram.

The simplified system model is shown in Figure 3 where the PMSM and rectifier are equivalent to a voltage source e, an internal resistor R_i and an internal inductor L_i. The internal inductance L_i is ignored to simplify the modelling [18] because the seat vibration energy is mainly at low frequency where the inductor can be treated as a conducting wire. The equivalent resistance of the external resistor and MOSFET switch is defined as:

$$R_E = D\frac{R_m R_e}{R_m + R_e} + (1 - D)R_e \quad (1)$$

where D is the value of the PWM duty cycle; R_m is the resistance within the MOSFET switch when it is turned on, which can be assumed to be zero Ohm. Thus, the equivalent resistance is:

$$R_E = (1 - D)R_e \quad (2)$$

The generated voltage is proportional to the rotary rate of the PMSM ω with a voltage constant k_e:

$$e = k_e\omega \quad (3)$$

The current i_p will make the PMSM generate a torque:

$$T_a = k_i i_p = k_i \frac{e}{R_i + R_E} = \frac{k_i k_e}{R_i + (1 - D)R_e}\omega \quad (4)$$

where k_i is the torque constant. And in the motor, we have $k_i = k_e$.

Then, the controllable rotary damping of the EMD system is:

$$c_r(t) = \frac{{k_i}^2}{R_i + (1 - D(t))R_e} \quad (5)$$

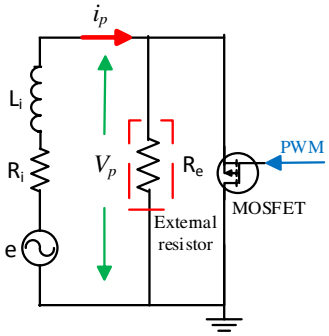

Figure 3. Simplified system model.

B. Test system

The test system is shown in Figure 4. A 400 W Panasonic servo motor, which can be accurately controlled by its drive, is used to rotate the EMD; thus, the EMD makes passive rotation. The encoder in the servo motor can be used to record the real rotation angle, and the applied torque of the servo motor can be taken as the torque output of the EMD. An NI CompactRio 9074 is applied to control the system and record data with different modules: an NI 9401 is used for controlling the servo motor and read the encoder data; the 10 V PWM signal is generated by an NI 9264 to control the MOSFET switch; an NI 9207 is used for acquiring servo motor's output torque from the drive of motor; an NI 9227 is used for measuring the current through the external resistor; and an NI 9239 is applied to measure the voltage V_p .

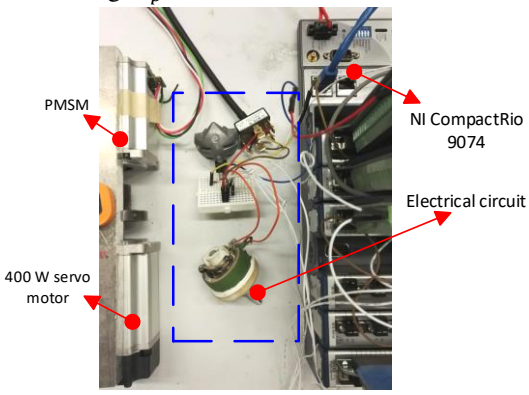

Figure 4. Test system for controllable EMD.

C. Constant rate rotation test

In order to analyse the EMD and control it, a series of tests are implemented. The servo motor drives the EMD to rotate in different constant rates (500 °/s, 1000 °/s, 1500 °/s, 2000 °/s, 2500 °/s), and its output torque is recorded with the PWM duty cycles varying from 0 to 1. Figure 5 shows that, with the same rotary rate, the output torque of EMD is increasing with the value of PWM duty cycle but is nonlinear. In Figure 6, when the PWM duty cycle is a constant value, the output torque is almost linear with the EMD rotary rate; in other words, the dampings of the EMD are constant values corresponding to certain PWM duty cycle values.

The slopes of lines in Figure 6 are calculated and taken as the damping of the EMD with corresponding PWM duty cycle values. Then the parameters for the controllable rotary damping of the EMD system in (5) are identified based on experimental results, which are shown in Table I where R_i actually includes the internal resistance of the motor and the resistance of three-phase rectifier. Figure 7 illustrates that the experimental and simulation results of the rotary damping are matched.

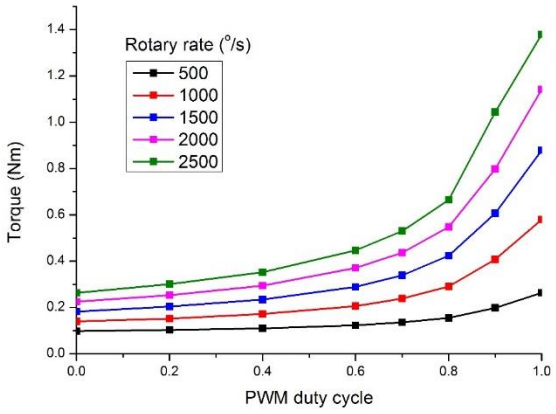

Figure 5. Torque output with PWM duty cycle variation

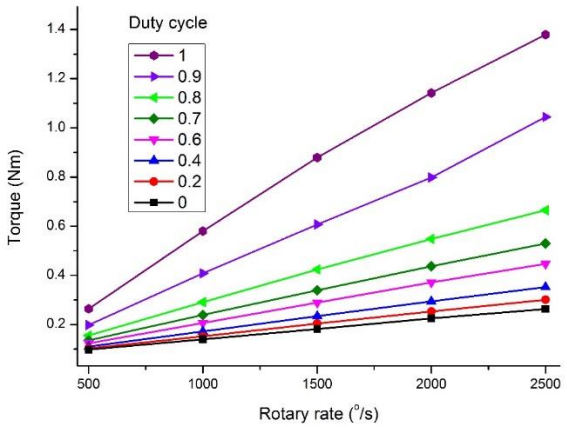

Figure 6. Torque output with PMSM rotary rate variation.

TABLE I
PARAMETERS IDENTIFICATION

Symbol	Value
$k_i(k_e)$	0.481 Nm/A (Vs/rad)
R_i	7.055 Ohm
R_e	40 Ohm

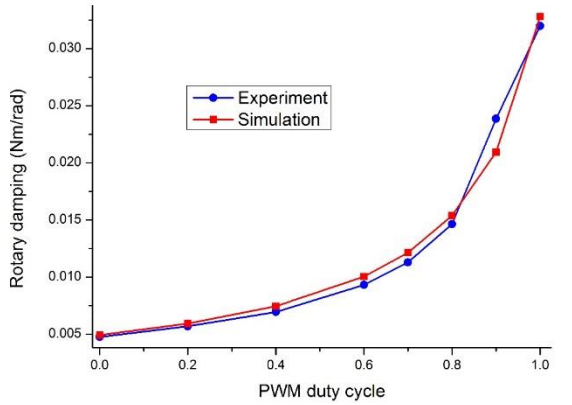

Figure 7. Rotary damping of the EMD.

Additionally, the equivalent external resistance is obtained from (5):

$$R_E = \frac{{k_i}^2}{c_r} - R_i \tag{6}$$

Figure 8 shows experiment result based on (6) and simulation result based on (2). The experiment proves that the equivalent external resistance is linear with the value of the PWM duty cycle.

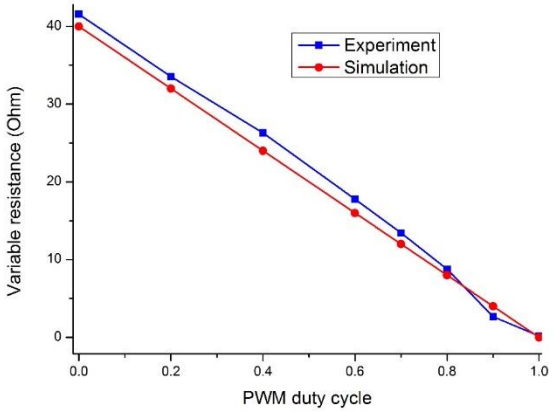

Figure 8. Equivalent external resistance.

D. Sinusoidal rotation test

The sinusoidal rotation test is also implemented. The servo motor drives the EMD to rotate with sinusoidal profile (with 1 Hz frequency, 300 ° amplitude). When PWM signal with different duty cycles is exerted on the MOSFET switch, the output torque of the EMD is varied (see Figure 9). The result indicates that the system damping can be controlled by varying PWM duty cycle; when the PWM duty cycle varies from 0 to 1, the damping is increasing.

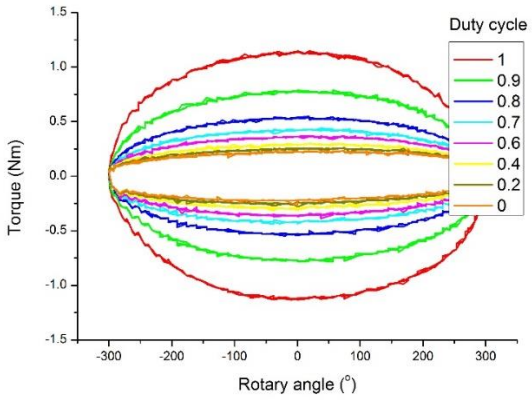

Figure 9. Rotary angle-torque.

The tested torque can be modelled as:

$$T_{at} = \frac{k_i k_e}{R_i + (1-D)R_e}\omega + F_{r0}\mathrm{sgn}(\omega) \tag{7}$$

where $F_{r0} \approx 0.045$ Nm is the identified rotary friction torque constant of the PMSM.

The comparison of experimental and simulation results are shown in Figure 10 where the results are very close to each other. It further indicates the correction of the model and the identified parameters, and the damping of the EMD can be accurately controlled with PWM signals.

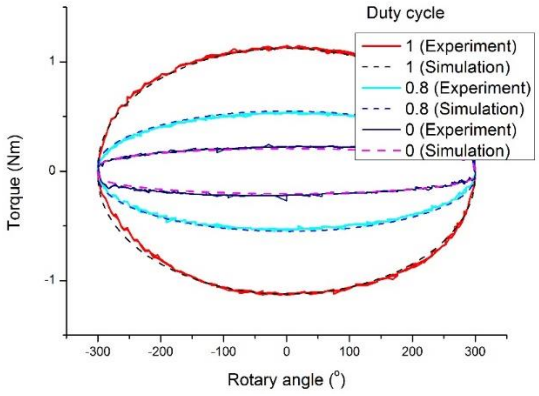

Figure 10. Comparison of experiment and simulation.

III. VARIABLE DAMPING SEAT SUSPENSION

The traditional variable damping seat suspensions, which apply the MR or ER dampers, need energy input to change the MR or ER fluid's viscosity, then the suspension damping can be controlled. A novel energy saving variable damping seat suspension system is presented in this section, which can be easily built by integrating a commercial passive seat suspension

and the controllable EMD. The whole system mathematical model has also been derived in the section.

A. Variable damping seat suspension

The designed variable damping seat suspension (see Figure 11) employs the original structure of a commercial passive seat suspension (GARPEN GSSC7); the proposed controllable EMD is installed in the centre of its scissors structure. In this design, no additional transmission devices (from linear motion to rotary one) are required as general regenerative suspension. A planetary gearbox is applied to amplify the torque output of the EMD (see Figure 12); the variable damper of the seat suspension consists of the gearbox and the EMD. In this paper, the gearbox ratio is selected as 20 which has been proven to be appropriate for a seat suspension in the following content.

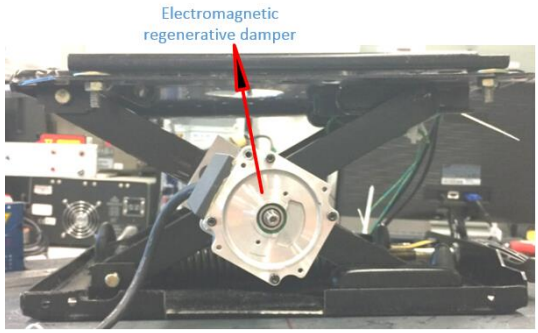

Figure 11. Variable damping seat suspension.

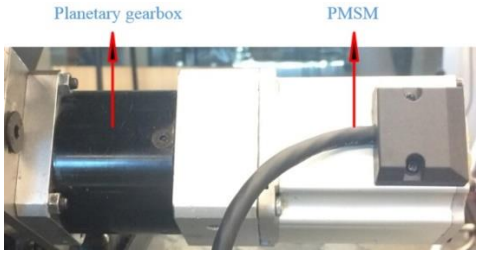

Figure 12. Prototype of the variable damper.

Figure 13 shows the kinematic model of the seat suspension where the damping torque T is transformed to a vertical force F by the scissors structure. The system energy flow is shown in Figure 14 where the kinematic energy from vibration goes through the scissors structure and gearbox to the EMD; damping torque generated by the EMD is amplified by the gearbox and then transformed to a vertical force F by the scissors structure. Based on the energy flow, the system model can be built.

The rotary angle of the scissors structure is:

$$\theta = 2\text{asin}(\frac{h_0 + h}{L}) \tag{8}$$

where $h_0 = 0.1$ m is the suspension initial height; h is the relative movement of suspension within vibration; $L = 0.287$ m is the length of the bar.

Then, we can obtain the rotary rate of the scissors structure:

$$\dot{\theta} = \frac{2\dot{h}}{\sqrt{L^2 - (h_0 + h)^2}} \tag{9}$$

The rotary rate of the EMD is:

$$\omega = r_g \dot{\theta} \tag{10}$$

where r_g is the gearbox ratio.

The torque generated by EMD is amplified by the gearbox, thus,

$$T = T_a r_g \tag{11}$$

By analysing the scissors structure, the equivalent force generated by the variable damper is:

$$F = \frac{2T}{\sqrt{L^2 - (h_0 + h)^2}} \tag{12}$$

Combining (4) and (8)-(12), the vertical force generated by the variable damper is:

$$F = \frac{4{r_g}^2{k_i}^2}{(L^2 - (h_0 + h)^2)(R_i + (1 - D)R_e)}\dot{h} \tag{13}$$

Thus, the variable damping of the seat suspension is:

$$c(t) = \frac{4{r_g}^2{k_i}^2}{(L^2 - \left(h_0 + h(t)\right)^2)(R_i + (1 - D(t))R_e)} \tag{14}$$

It is easy to know that the damping of the seat suspension is controlled by the value of PWM duty cycle, and is related to the selection of gearbox, the torque or voltage constant of the PMSM, the internal and external resistances, the relative displacement, and the parameters of the seat suspension.

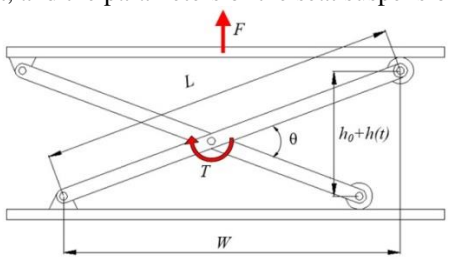

Figure 13. Kinematic model of seat suspension.

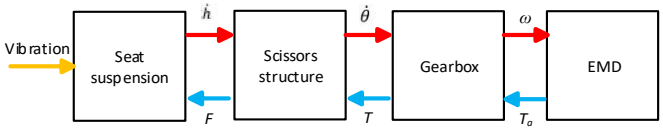

Figure 14. Energy flow.

B. System analysis

The controllable seat suspension damping is defined in (14), where the damping is determined by the PWM signal D and the suspension deflection h. By assuming that the seat suspension deflection is within -0.01 m and 0.01 m, the seat suspension damping is shown in Figure 15 which indicates that the seat suspension damping can be controlled by the PWM signal and is slightly related to the suspension deflection. The damping of the seat suspension can continuously vary from 112 Ns/m to 746 Ns/m. This variation range of damping has been proven suitable for the seat suspension in the experiment; it can successfully suppress the high magnitude resonance vibration with the large damping and provide good ride comfort in high frequency vibration with the small damping.

The EMD transforms the vibration energy into electrical energy which is then consumed by the internal resistance R_i and external resistance R_e. The part of energy consumed by the external resistor is the harvestable energy. Therefore, the energy harvest efficiency of the system is [28]:

$$\eta = \frac{{i_p}^2 R_E}{{i_p}^2 (R_i + R_E)} = \frac{(1-D)R_e}{R_i + (1-D)R_e} \tag{15}$$

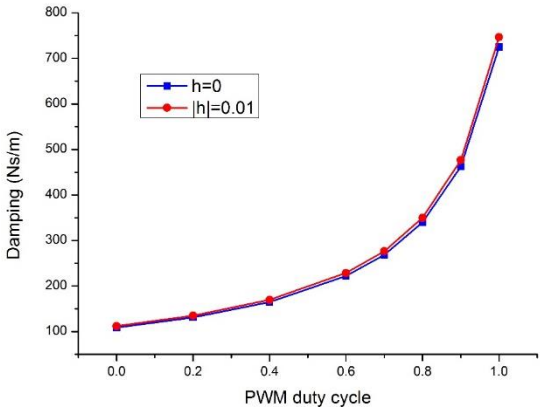

Figure 15. Controllable seat suspension damping with different suspension deflections.

Figure 16 shows the energy harvest efficiency with external resistance 40 Ohm and 10 Ohm, respectively. It is noted that the higher resistance value of the external resistor will lead to higher energy harvest efficiency. In Figure 17, with a higher value of the external resistance, the seat suspension will have a lower smallest damping; with a lower value of external resistance, the relationship between the damping and PWM duty cycle tends to be linear.

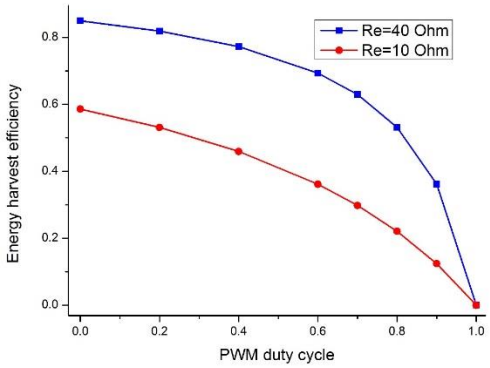

Figure 16. Energy harvest efficiency.

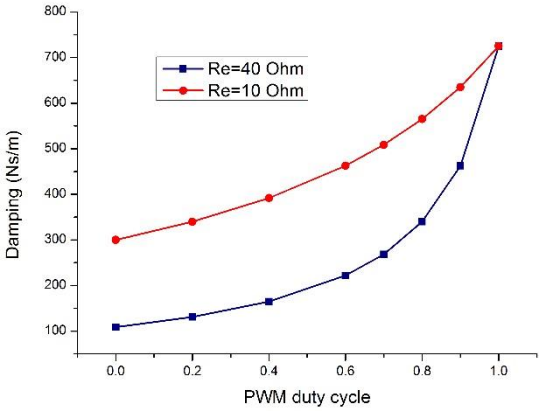

Figure 17. Seat suspension damping with different external resistances when $h = 0$.

Several parameters determine the controllable damping of the seat suspension. Generally, the suspension parameters L and h_0, the voltage (torque) constant k_e (k_i) and internal resistance R_i are hard to be modified. By replacing the gearbox with different ratios and the external resistor with different resistances, the range of the variable damping can be optimised for seat suspension in different work scenarios.

IV. CONTROLLER DESIGN

In this section, an implementable control method is proposed for the variable damping seat suspension.

The simplified seat suspension model is shown in Figure 18 where m is the mass loaded on the suspension; k is the suspension stiffness; c is the controllable damping; f_r is the friction; z_s is the seat displacement and z_v is the cabin floor displacement.

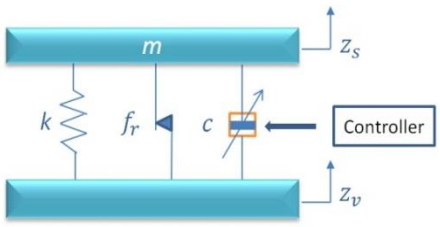

Figure 18. Seat suspension model.

The seat suspension model is defined as:

$$m\ddot{z}_s = -k(z_s - z_v) + u - f_r \tag{16}$$

$$u = -\frac{4{r_g}^2 {k_i}^2 (\dot{z}_s - \dot{z}_v)}{(L^2 - (h_0 + z_s - z_v)^2)(R_i + (1 - D(t))R_e)} \tag{17}$$

For designing a controller, the state variables are chosen as $x_1 = z_s - z_v$, $x_2 = \dot{z}_s$. There are two disturbances, i.e., $d_1 = -\dot{z}_v$, $d_2 = -f_r$. Thus, the suspension model can be written as a state space form:

$$\dot{\mathbf{X}} = \mathbf{A}\mathbf{X} + \mathbf{B_1}\boldsymbol{\omega} + \mathbf{B_2}u \tag{18}$$

where $\mathbf{X} = [x_1\ x_2]^{\mathrm{T}}$, $\mathbf{A} = \begin{bmatrix} 0 & 1 \\ -\frac{k}{m} & 0 \end{bmatrix}$, $\mathbf{B_1} = \begin{bmatrix} 1 & 0 \\ 0 & \frac{1}{m} \end{bmatrix}$, $\boldsymbol{\omega} = [d_1\ d_2]^{\mathrm{T}}$, $\mathbf{B_2} = [0\ \frac{1}{m}]^{\mathrm{T}}$.

For the seat suspension control, the driver comfort is the most importance criterion. Therefore, the controlled output, the acceleration of the driver body, is defined as:

$$z = \mathbf{C_1}\mathbf{X} + \mathbf{D_{11}}\boldsymbol{\omega} + \mathrm{D}_{12}u \tag{19}$$

where $\mathbf{C_1} = \left[-\frac{k}{m}\quad 0\right]$, $\mathbf{D_{11}} = \left[0\quad \frac{1}{m}\right]$, $\mathrm{D}_{12} = \frac{1}{m}$.

The proposed seat suspension can only be semi-actively controlled, thus the desired control force of a controller cannot be fully implemented. This kind of output saturation will affect the performance of observer based controllers. The sliding mode controller is robust to the disturbance, but its sliding surface may be hard to be accurately defined for a semi-actively controlled system with uncertainties. The H_∞ controller is highly robust to uncertainties and has the capability to deal with the disturbance induced by output saturation. In addition, it is easy to be integrated with the proposed controller implementation method, thus the H_∞ controller is chosen for this system.

A state feedback H_∞ controller can be designed as:

$$u = \mathbf{KX} \tag{20}$$

where $\mathbf{K}$ is the feedback gain to be designed.

The $\mathcal{L}_2$ gain of the system (18) and (19) is defined as:

$$\|T_{Z\boldsymbol{\omega}}\|_\infty = \sup \frac{\|z\|_2}{\|\boldsymbol{\omega}\|_2} \quad (\|\boldsymbol{\omega}\|_2 \neq 0) \tag{21}$$

where $\|z\|_2 = \int_0^\infty z^{\mathrm{T}}(t)z(t)\mathrm{d}t$ and $\|\boldsymbol{\omega}\|_2 = \int_0^\infty \boldsymbol{\omega}^{\mathrm{T}}(t)\boldsymbol{\omega}(t)\mathrm{d}t$.

It is easy to conclude that if there is a positive definite matrix $\mathbf{P} = \mathbf{P}^{\mathbf{T}} > 0$, such that the following linear matrix inequality (LMI) is satisfied [29]:

$$\in = \begin{bmatrix} * & + \mathbf{P}(\mathbf{A} + \mathbf{B_2 K}) & * & * \\ & \mathbf{B_1}^{\mathbf{T}}\mathbf{P} & -\lambda^2\mathbf{I} & * \\ & \mathbf{C_1} + \mathrm{D}_{12}\mathbf{K} & \mathbf{D_{11}} & -\mathbf{I} \end{bmatrix} < 0 \tag{22}$$

then the system (21) is stable with H_∞ performance index $\lambda > 0$.

Pre- and post-multiplying (22) by diag($\mathbf{P^{-1}}, \mathbf{I}, \mathbf{I}$) and its transpose, respectively, and defining $\mathbf{Q} = \mathbf{P^{-1}}$, $\mathbf{KQ} = \mathbf{Y}$, the condition $\in < 0$ is equivalent to

$$\exists = \begin{bmatrix} * & + \mathbf{AQ} + \mathbf{B_2 Y} & * & * \\ & \mathbf{B_1}^{\mathbf{T}} & -\lambda^2\mathbf{I} & * \\ & \mathbf{C_1 Q} + \mathrm{D}_{12}\mathbf{Y} & \mathbf{D_{11}} & -\mathbf{I} \end{bmatrix} < 0 \tag{23}$$

By solving (23) for $\mathbf{Y}$ and $\mathbf{Q}$, the controller gain is obtained as $\mathbf{K} = \mathbf{YQ^{-1}}$. By applying the parameters in Table II, $\mathbf{K} = [4899 \quad -185]$ is calculated in this paper.

TABLE II
PARAMETERS FOR CONTROLLER DESIGN

Symbol	Value
k	5000 N/m
m	80 Kg
λ	1.22

When the desired active control force is achieved, the desired damping of seat suspension is:

$$c_d = \begin{cases} -\dfrac{u}{\dot{x}_1} & (\dot{x}_1 \neq 0) \\ c_{max} & (\dot{x}_1 = 0) \end{cases} \tag{24}$$

where c_{max} is the maximum damping that the damper can generate. When $\dot{x}_1 = 0$, there is no force output from the damper, therefore, c_d can be an arbitary value.

However, the damping of the seat suspension can only vary between the minimum damping c_{min} and the maximum c_{max}. They are defined as:

$$c_{min} = \frac{4{r_g}^2{k_i}^2}{(L^2 - (h_0 + \dot{x}_1)^2)(R_i + R_e)} \tag{25}$$

$$c_{max} = \frac{4{r_g}^2{k_i}^2}{(L^2 - (h_0 + \dot{x}_1)^2)R_i} \tag{26}$$

If c_d is within c_{min} and c_{max}, the value of the desired PWM duty cycle is:

$$D = 1 + \frac{4{r_g}^2{k_i}^2\dot{x}_1}{(L^2 - (h_0 + x_1)^2)uR_e} + \frac{R_i}{R_e} \tag{27}$$

If $c_d < c_{min}$, it means that the desired force can only be generated by an active actuator; the variable damper cannot meet the requirement, therefore, $D = 0$ is applied.

If $c_d > c_{max}$, it means that the desired damping is larger than the maxium damping that the variable damper can generate, thus $D = 1$ is applied.

The implementation of the controller can be seen in Figure 19, which is very straightforward.

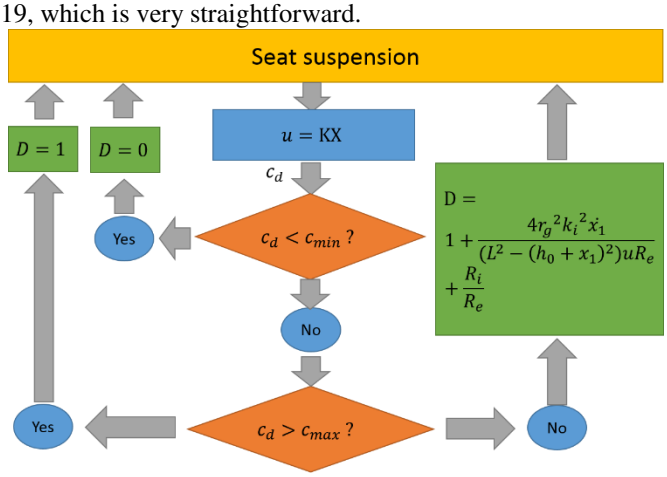

Figure 19. Controller implementation.

V. EVALUATION

A. Experimental setup

The experimental setup is shown in Figure 20. The variable damping seat suspension is mounted on a 6-degree of freedom (6-DOF) vibration platform which is under the control of an NI CompactRio 9076; the vibration platform can generate desired vibration based on the commands from Computer 2. The relative displacement of the seat suspension is measured by a laser sensor (Micro Epsilon optoNCDT 1700); and another laser sensor is applied to measure the displacement of the top platform of the seat suspension. Two acceleration sensors (ADXL 203EB) are used to obtain the top and base accelerations of the seat suspension. An NI CompactRio 9074 is used to control a MOSFET switch based on sensors' feedback.

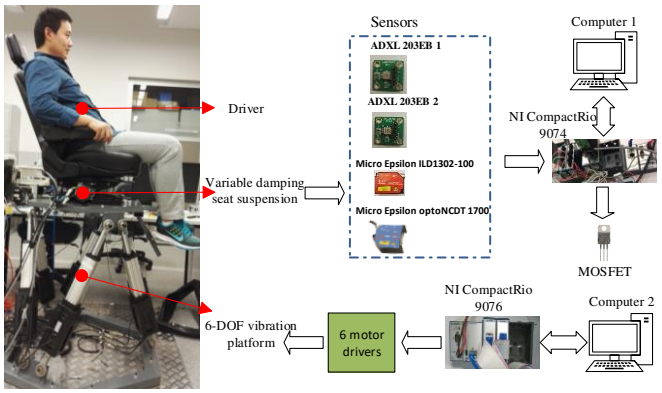

Figure 20. Experimental setup.

For evaluating the vibration control performance of the variable damping seat suspension, a well tuned commercial passive seat suspension (GARPEN GSSC7) is also tested; it is the same type of seat suspension that has been modified to the variable damping seat suspension.

B. Acceleration transmissibility

The acceleration transmissibility can show the performance of a seat suspension in frequency domain; lower transmissibility value means less acceleration can be transferred to driver from seat base. By exerting different

frequencies of vibration on the base of the seat suspension, the root mean square (RMS) accelerations of the seat suspension top and base are caculated; then, the transmissibility of RMS acceleration, which is shown in Figure 21, can be obtained by using RMS acceleration of the top devided by the one of base. The seat suspension with the smallest damping ($D = 0$) has a peak value around 1.4 Hz which is the resonance frequency of the seat suspension; when $D = 1$, the resonance peak is suppressed but the transmissibility in the high frequency has larger values. The conventional passive seat suspnesion has a higher transmissibility than the maximum damping one around resounance frequency, and has a lower transmissibility with 4 Hz vibration. The result indicates that the damping of the conventional passive seat suspnesion is within the maximun and minimum damping of the proposed seat suspnsion. When the variable damping seat suspension is controlled, it has similar performance with the conventional seat suspnesion with vibration lower than 1.4 Hz, and in high frequency, its performance is close to the smallest damping seat suspension. The experiment result implies that the controlled variable damping seat suspension can effectively suppress the resonance vibration, and is capable to isolate the high frequency vibration.

Figure 22 shows the output PWM duty cycle, and Figure 23 shows the desired active force and the actual semi-active control ouput force. The noncoincidental part of the force is happened in the time when the damper cannot generate the desired active force.

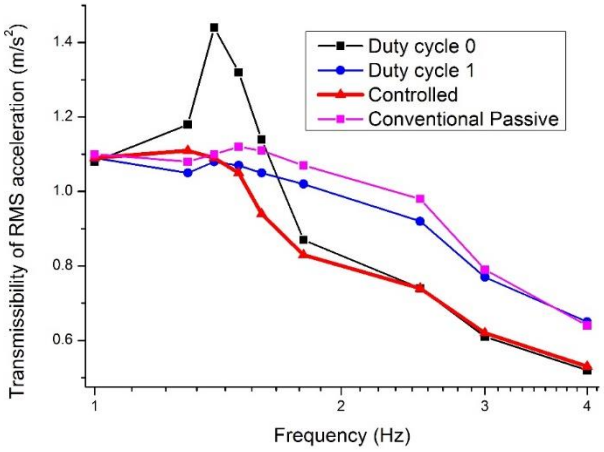

Figure 21. Transmissibility.

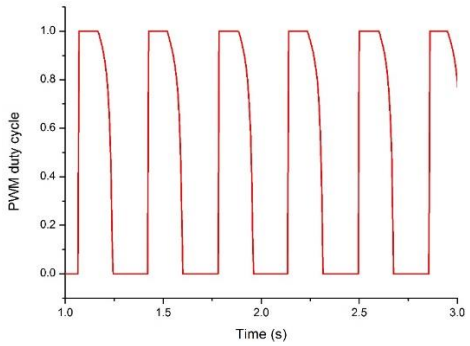

Figure 22. PWM duty cycle at 1.4 Hz vibration.

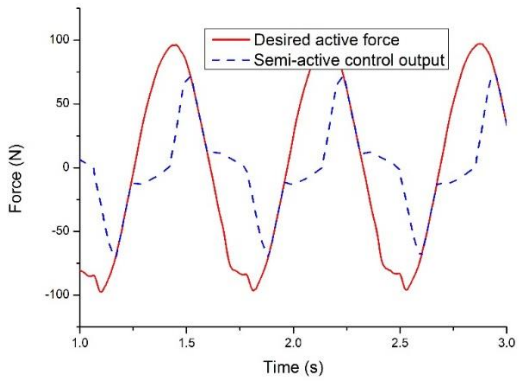

Figure 23. Force at 1.4 Hz vibration.

C. Random vibration test

For evaluating its time domain performance, the random excitation test is implemented. The random vibration profile is generated through a quarter-car model under random road profile input, which is a typical road condition used to test suspension performance. The displacement of the sprung mass of the quarter-car model is taken as the vibration input to the seat suspension.

Figure 24 shows the seat acceleration of the controlled variable damping seat suspension and the proposed seat suspension with maximum and minimum damping. The performance comparison with the conventional passive seat suspension is shown in Figure 25. It is easy to see that there is high peak acceleration when the damping of the seat suspension is low, and the high damping seat suspension can effectively suppress the resonance vibration but has high vibration magnitudes in other area. Obviously, the controlled variable damping seat suspension has the best performance.

The PWM duty cycle output of the proposed seat suspension system is shown in Figure 26, and corresponding force output is shown in Figure 27. By controlling the PWM duty cycle, the variable damper is varying the damping to generate a semi-active force which can meet about 40% of the requirement of the desired active force.

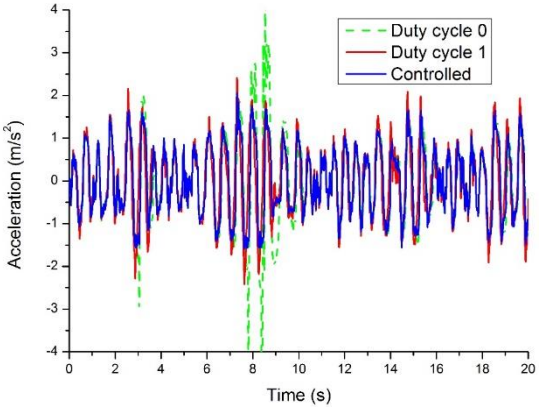

Figure 24. Acceleration comparison with different damping seat suspension.

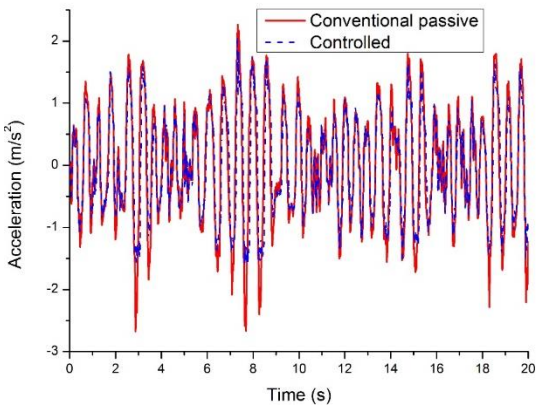

Figure 25. Acceleration comparison with the conventional passive seat suspension

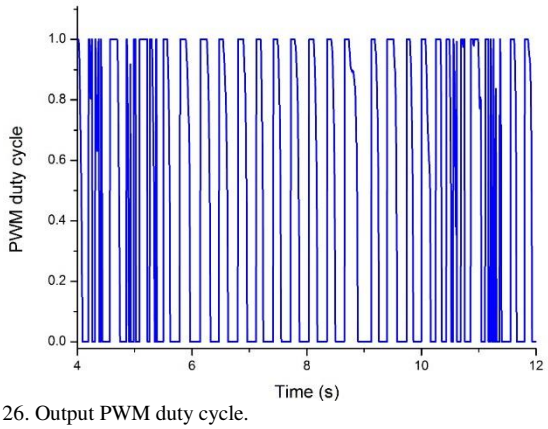

Figure 26. Output PWM duty cycle.

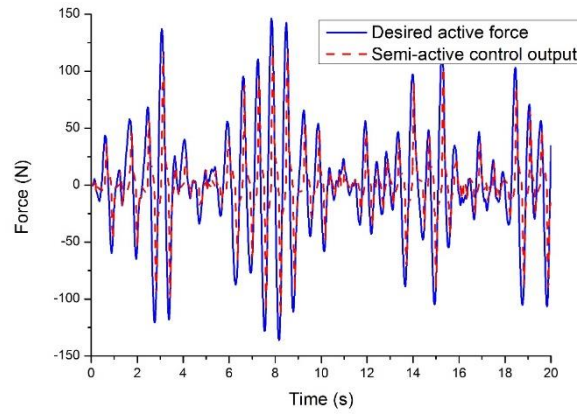

(a)

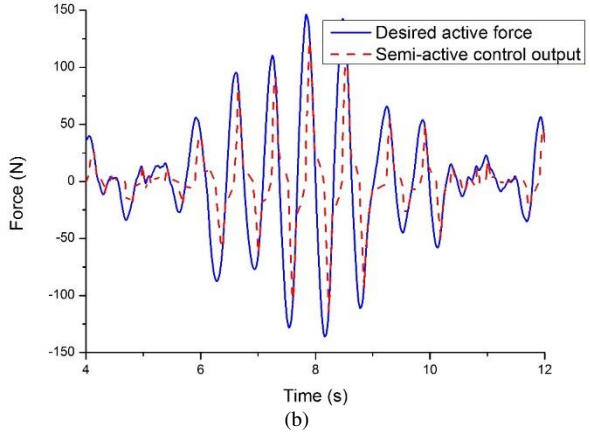

(b)

Figure 27. Generated force.

In order to analyse the seat suspension performance quantitatively, an international standard ISO 2631-1 [30] is applied to evaluate it. The frequency weighted RMS (FW-RMS) acceleration and the fourth power vibration dose value (VDV) are obtained based on the guideline of ISO 2631-1. The FW-RMS acceleration is always applied to evaluate the ride comfort, because it is calculated by referring that human body has different response to different vibration frequency. The VDV is more sensitive to the peak vibration; it is an additional evaluation of vibration. According to the international standard, the two evaluation parameters are defined as:

$$a_{\mathrm{FW-RMS}} = [\frac{1}{\mathrm{T}}\int_0^{\mathrm{T}} \{a_{\mathrm{FW-RMS}}(\mathrm{t})^2 \mathrm{dt}\}]^{1/2} \quad (28)$$

$$\mathrm{VDV} = [\int_0^{\mathrm{T}} \{a_{\mathrm{w}}(\mathrm{t})^4 \mathrm{dt}\}]^{1/4} \quad (29)$$

Figure 28 shows the value of the evaluation parameters where the RMS acceleration, FW-RMS acceleration and VDV are decreased by 17.2%, 13.9% and 19.7%, respectively, when compared with the conventional passive one; when compared with the low damping case (D = 0), the decreases reach to 25.6%, 26.5% and 53.8%, respectively.

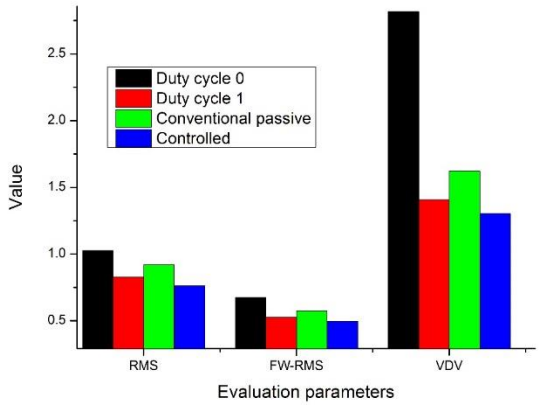

Figure 28. Evaluation parameters.

The current (i_0) through the external resistor R_e is recorded in the experiment, therefore, harvestable power can be calculated by:

$$\mathrm{P} = {i_0}^2 R_e \quad (30)$$

Figure 29 shows the harvestable power when the proposed seat suspension is controlled. The maximum power can be over 25 W with short period of time, and the RMS power is 1.492 W. In this paper, the rotary motor is applied to harvest energy, which can generate more power than the method with linear motors [20, 22] when the devices have same volumes. The variable damping seat suspension is controlled by PWM signal whose energy consumption can be ignored when compared with the energy harvesting potential. If energy storage devices, such as the battery and supercapacitor, are introduced to the system, the system can work without energy provision from vehicle battery.

Additionally, the application of this seat suspension can be extended: when the vehicle is working on roads with different roughness, corresponding damping can be selected by exerted different PWM signals, thus, real-time control is not required and fewer sensors are needed.

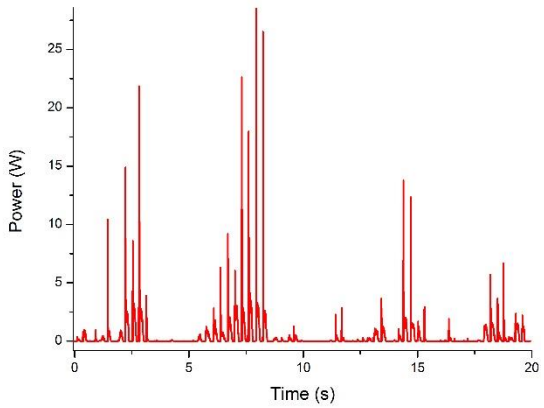

Figure 29. Harvestable power.

VI. CONCLUSIONS

In this work, a continuously variable damping seat suspension with an EMD has been designed, manufactured and evaluated; the proposed seat suspension is energy saving when compared with other variable damping seat suspension with MR or ER damper, and it has regeneration capability. A commercial passive seat suspension has been modified by removing its original damper and installing the variable damper in the centre of its scissors structure to build a variable damping seat suspension. A test system has been designed to analyse the variable damping characteristics of the EMD system. The test result indicates that the damping of the EMD can be continuously controlled by exerting different PWM signals on the MOSFET switch. Based on the test results, the model parameters of the EMD system have been identified. By analysing the kinematics of the seat suspension, it is known that the damping of the seat suspension can continuously vary from 112 Ns/m to 746 Ns/m. Then, a control method for vibration isolation has been designed for the seat suspension prototype. The designed seat suspension and its control method have been validated with vibration test on a 6-DOF vibration platform. When the variable damping seat suspension is controlled, the RMS acceleration, FW-RMS acceleration and VDV are decreased by 17.2%, 13.9% and 19.7%, respectively, when compared with the conventional passive one. The RMS harvestable power reaches 1.492W. The energy consumption of the PWM control signal is ignorable. Therefore, this energy saving variable damping seat suspension is promising in the application, especially for the future electric vehicles. In the future, more system characteristics, such as electrical networks with different combinations of electrical components, need to be explored, higher performance controllers are going to be developed, and the energy storage circuit needs to be integrated into the system.

REFERENCES

[1] I. M. Virtanen *et al.*, "Occupational and genetic risk factors associated with intervertebral disc disease," *Spine,* vol. 32, no. 10, pp. 1129-1134, 2007.

[2] T. D. Le and K. K. Ahn, "A vibration isolation system in low frequency excitation region using negative stiffness structure for vehicle seat," *Journal of Sound and Vibration,* vol. 330, no. 26, pp. 6311-6335, 2011.

[3] Z. Gan, A. J. Hillis, and J. Darling, "Adaptive control of an active seat for occupant vibration reduction," *Journal of Sound and Vibration,* vol. 349, pp. 39-55, 2015.

[4] I. Maciejewski, L. Meyer, and T. Krzyzynski, "The vibration damping effectiveness of an active seat suspension system and its robustness to varying mass loading," *Journal of Sound and Vibration,* vol. 329, no. 19, pp. 3898-3914, 2010.

[5] K. K. Ahn, "Active pneumatic vibration isolation system using negative stiffness structures for a vehicle seat," *Journal of Sound and Vibration,* vol. 333, no. 5, pp. 1245-1268, 2014.

[6] D. Ning, S. Sun, H. Li, H. Du, and W. Li, "Active control of an innovative seat suspension system with acceleration measurement based friction estimation," *Journal of Sound and Vibration,* vol. 384, pp. 28-44, 12/8/ 2016.

[7] D. Ning, S. Sun, F. Zhang, H. Du, W. Li, and B. Zhang, "Disturbance observer based Takagi-Sugeno fuzzy control for an active seat suspension," *Mechanical Systems and Signal Processing,* vol. 93, pp. 515-530, 2017.

[8] M. Kawana and T. Shimogo, "Active suspension of truck seat," *Shock and vibration,* vol. 5, no. 1, pp. 35-41, 1998.

[9] S.-B. Choi and Y.-M. Han, "Vibration control of electrorheological seat suspension with human-body model using sliding mode control," *Journal of Sound and Vibration,* vol. 303, no. 1, pp. 391-404, 2007.

[10] S.-B. Choi, M.-H. Nam, and B.-K. Lee, "Vibration control of a MR seat damper for commercial vehicles," *Journal of Intelligent Material Systems and Structures,* vol. 11, no. 12, pp. 936-944, 2000.

[11] S. Sun, D. Ning, J. Yang, H. Du, S. Zhang, and W. Li, "A seat suspension with a rotary magnetorheological damper for heavy duty vehicles," *Smart Materials and Structures,* vol. 25, no. 10, p. 105032, 2016.

[12] G. J. Hiemenz, W. Hu, and N. M. Wereley, "Semi-active magnetorheological helicopter crew seat suspension for vibration isolation," *Journal of Aircraft,* vol. 45, no. 3, pp. 945-953, 2008.

[13] F. Khoshnoud, D. B. Sundar, M. Badi, Y. K. Chen, R. K. Calay, and C. W. De Silva, "Energy harvesting from suspension systems using regenerative force actuators," *International Journal of Vehicle Noise and Vibration,* vol. 9, no. 3-4, pp. 294-311, 2013.

[14] R. Wang, R. Ding, and L. Chen, "Application of hybrid electromagnetic suspension in vibration energy regeneration and active control," *Journal of Vibration and Control,* p. 1077546316637726, 2016.

[15] L. Zuo and P.-S. Zhang, "Energy harvesting, ride comfort, and road handling of regenerative vehicle suspensions," *Journal of Vibration and Acoustics,* vol. 135, no. 1, p. 011002, 2013.

[16] L. Pires, M. Smith, N. Houghton, and R. McMahon, "Design trade-offs for energy regeneration and control in vehicle suspensions," *International Journal of Control,* vol. 86, no. 11, pp. 2022-2034, 2013.

[17] Y. M. Roshan, A. Maravandi, and M. Moallem, "Power electronics control of an energy regenerative mechatronic damper," *IEEE Transactions on Industrial Electronics,* vol. 62, no. 5, pp. 3052-3060, 2015.

[18] Z. Li, L. Zuo, G. Luhrs, L. Lin, and Y.-x. Qin, "Electromagnetic energy-harvesting shock absorbers: design, modeling, and road tests," *IEEE Transactions on Vehicular Technology,* vol. 62, no. 3, pp. 1065-1074, 2013.

[19] Z. Zhang *et al.*, "A high-efficiency energy regenerative shock absorber using supercapacitors for renewable energy applications in range extended electric vehicle," *Applied Energy,* vol. 178, pp. 177-188, 2016.

[20] L. Zuo, B. Scully, J. Shestani, and Y. Zhou, "Design and characterization of an electromagnetic energy harvester for vehicle suspensions," *Smart Materials and Structures,* vol. 19, no. 4, p. 045003, 2010.

[21] S. Zhu, W.-a. Shen, and Y.-l. Xu, "Linear electromagnetic devices for vibration damping and energy harvesting: Modeling and testing," *Engineering Structures,* vol. 34, pp. 198-212, 2012.

[22] X. Tang, T. Lin, and L. Zuo, "Design and optimization of a tubular linear electromagnetic vibration energy harvester," *IEEE/ASME Transactions on Mechatronics,* vol. 19, no. 2, pp. 615-622, 2014.

[23] A. Gupta, J. Jendrzejczyk, T. Mulcahy, and J. Hull, "Design of electromagnetic shock absorbers," *International Journal of Mechanics and Materials in Design,* vol. 3, no. 3, pp. 285-291, 2006.

[24] Z. Jin-qiu, P. Zhi-zhao, Z. Lei, and Z. Yu, "A review on energy-regenerative suspension systems for vehicles," in

Proceedings of the World Congress on Engineering, 2013, vol. 3, pp. 3-5.
[25] Y. Zhang, H. Chen, K. Guo, X. Zhang, and S. E. Li, "Electro-hydraulic damper for energy harvesting suspension: Modeling, prototyping and experimental validation," *Applied Energy,* vol. 199, pp. 1-12, 2017.
[26] B. Sapiński, "Energy-harvesting linear MR damper: prototyping and testing," *Smart Materials and Structures,* vol. 23, no. 3, p. 035021, 2014.
[27] S. Choi, M. Seong, and K. Kim, "Vibration control of an electrorheological fluid-based suspension system with an energy regenerative mechanism," *Proceedings of the Institution of Mechanical Engineers, Part D: Journal of Automobile Engineering,* vol. 223, no. 4, pp. 459-469, 2009.
[28] C. Lv, J. Zhang, Y. Li, and Y. Yuan, "Mechanism analysis and evaluation methodology of regenerative braking contribution to energy efficiency improvement of electrified vehicles," *Energy Conversion and Management,* vol. 92, no. Supplement C, pp. 469-482, 2015/03/01/ 2015.
[29] H. Li, J. Yu, C. Hilton, and H. Liu, "Adaptive sliding-mode control for nonlinear active suspension vehicle systems using T–S fuzzy approach," *IEEE Transactions on Industrial Electronics,* vol. 60, no. 8, pp. 3328-3338, 2013.
[30] ISO, "Mechanical Vibration and Shock – Evaluation of Human Exposure to Whole-body Vibration – Part 1: General Requirements," *ISO 2631–1,* 1997.

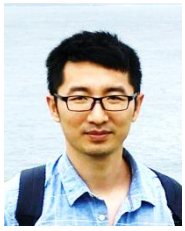

Donghong Ning received the B.E. degree in agricultural mechanization and automation from the College of Mechanical and Electronic Engineering, North West Agriculture and Forestry University, Yangling, China, in 2012 and PhD degree in 2018 from University of Wollongong, Australia. He is currently working as an associate research fellow at the School of Electrical, Computer and Telecommunications Engineering, University of Wollongong, Wollongong, N.S.W., Australia. His research interests include seat suspension vibration control and multiple degrees of freedom vibration control.

Haiping Du (M'09-SM'17) received the Ph.D. degree in mechanical design and theory from Shanghai Jiao Tong University, Shanghai, China, in 2002. He was a Research Fellow with the University of Technology, Sydney, from 2005 to 2009, and was a Postdoctoral Research Associate with Imperial College London from 2004 to 2005 and the University of Hong Kong from 2002 to 2003. He is currently a Professor at the School of Electrical, Computer and Telecommunications Engineering, University of Wollongong, Wollongong, N.S.W, Australia. He is a Subject Editor of the Journal of Franklin Institute, an Associate Editor of IEEE Control Systems Society Conference, an Editorial Board Member for some international journals, such as Journal of Sound and Vibration, IMechE Journal of Systems and Control Engineering, Journal of Low Frequency Noise, Vibration and Active Control, and a Guest Editor of IET Control Theory and Application, Mechatronics, Advances in Mechanical Engineering, etc. His research interests include vibration control, vehicle dynamics and control systems, robust control theory and engineering applications, electric vehicles, robotics and automation, smart materials and structures. He is a recipient of the Australian Endeavour Research Fellowship (2012).

.

Shuaishuai Sun received the B.E. degree in mechanical engineering and automation from the China University of Mining and Technology, Beijing, China, in 2011, and PhD degree in 2016 from University of Wollongong, Australia. He is currently working as a research fellow at the School of Mechanical, Material and Mechatronics Engineering, University of Wollongong, Wollongong, N.S.W, Australia. His research interests include self-sensing self-power MR devices, smart materials and structures, innovative actuators for locomotive robot, and vibration control. He has published more than 40 journal articles in his research field.

Wenfei Li was born in Qingyatou Village, Yangquan City, in 1988. He received the B.E. and M.S. degrees in mechanical engineering and automation from the China University of Mining and Technology, Beijing, in 2011. He is currently working toward his Ph.D. on brake-by-wire vehicle control at the School of Electrical, Computer and Telecommunications Engineering at the University of Wollongong, Australia.

Weihua Li (M'15) received the B.E. and M.E. degrees from the University of Science and Technology of China, Hefei, China, in 1992 and 1995, respectively, and the Ph.D degree from Nanyang Technological University, Nanyang, Singapore, in 2001. He was with the school of Mechanical and Production Engineering, Nanyang Technological University, as a Research Fellow, from 2001 to 2003. He has been with the School of Mechanical, Materials and Mechatronic Engineering, University of Wollongong, Wollongong, N.S.W, Australia, as an Academic Staff Member, since 2003. He has published more than 320 technical articles in refereed international journals and conferences. He serves as an Associate Editor or Editorial Board Member for ten international journals. Dr. Li received the number of awards, including Fellow of the Institute of Engineers Australia, Fellow of the Institute of Physics, UK, the JSPS Invitation Fellowship in 2014, the Endeavour Research Fellowship in 2011, and the Scientific Visits to China Program Awards.